RNA-seq screening and gene function analysis uncover GPR183 as a key mediator for methionine to stimulate milk synthesis in mouse mammary epithelial cells

Yuwen Zhou, Sihua Fan, Ming Xu, Minghui Zhang*, Xuejun Gao*

College of Animal Science and Technology, Yangtze University, Jingzhou, 434025, China

***Corresponding author:** Minghui Zhang, Tel and Fax: +86-716-8066256; E-mail: minghuizhang2019@163.com; ORCID: 0000-0002-8253-1379. Xuejun Gao, Tel and Fax: +86-716-8066256; E-mail: gaoxj53901@163.com. ORCID: 0000-0002-8241-6346.

Short running head: GPR183 mediates methionine stimulation on milk synthesis

ABBREVIATIONS:
DEGs; differentially expressed genes
FBS; fetal bovine serum
GO; Gene Ontology
GPCR; G protein-coupled receptor
KEGG; The Kyoto Encyclopedia of Genes and Genomes
MECs; mammary epithelial cells
Met; Methionine
mTOR; the mechanistic target of rapamycin
PI3K; phosphoinositide 3-kinase
sgRNA; single-guide RNA
TGs; triglycerides

This peer-reviewed article has been accepted for publication but not yet copyedited or typeset, and so may be subject to change during the production process. The article is considered published and may be cited using its DOI
10.1017/S0007114524001223
The British Journal of Nutrition is published by Cambridge University Press on behalf of The Nutrition Society

Abstract

Methionine (Met) can activate mTOR to promote milk synthesis in mammary epithelial cells (MECs). However, it is largely unknown which G protein-coupled receptor (GPCR) can mediate the stimulation of Met on mTOR activation. In this study, we employed transcriptome sequencing to analyze which GPCRs were associated with the role of Met, and further used gene function study approaches to explore the role of GPR183 in Met stimulation on mTOR activation in HC11 cells. We identified 9 GPCRs including GPR183 which expression levels were upregulated by Met treatment through RNA-seq and subsequent RT-qPCR analysis. Using GPR183 knockdown and overexpression technology, we demonstrate that GPR183 is a positive regulator of milk protein and fat synthesis and proliferation of HC11 cells. Met affected GPR183 expression in a dose-dependent manner, and GPR183 mediated the stimulation of Met (0.6 mM) on milk protein and fat synthesis, cell proliferation, and mTOR phosphorylation and mRNA expression. The inhibition of PI3K blocked the phosphorylation of mTOR and AKT stimulated by GPR183 activation. In summary, through RNA-seq and gene function study, we uncover that GPR183 is a key mediator for Met to activate the PI3K-mTOR signaling and milk synthesis in mouse MECs.

Keywords: GPR183, mammary epithelial cell, Methionine, mTOR, RNA-seq

Introduction

Milk, as a high-protein and fat food, is the only food for newborn mammals and a very important food for people. Milk protein and fat are synthesized and secreted by mammary epithelial cells (MECs), which are the functional units of mammary glands[1]. The quantity of MECs directly influences volume of milk secreted by mammary glands, and the milk synthesis ability and proliferative state of MECs in the lactation stage of mammary gland are influenced by hormones and nutrients such as amino acids[2,3,4].

The mechanistic target of rapamycin (mTOR), a conserved Ser/Thr protein kinase, serves as a main signaling hub in regulating protein and lipid synthesis and cell proliferation[5,6]. mTOR can enhance or attenuate diverse cellular metabolic processes in responding to nutrients and various other growth signals[7]. Amino acids are required for mTOR activation, and exerts significant influence on cell metabolism and proliferation[5]. It has been established that mTOR is the central regulator of milk synthesis and proliferation of MECs, and amino acids can promote milk synthesis through activating mTOR[8.9].

G-protein coupled receptors (GPCRs), a large profoundly conserved protein superfamily, have seven transmembrane α-helical structure, and can perceive a myriad of extracellular stimuli including hormones, growth factors, amino acids, etc.[10] These signals can bind to the extracellular N-terminal domain of certain GPCR, and thereby change the conformation of its intracellular C-terminal domain and thereby transduce extracellular signals to trimeric G-proteins and their downstream effectors such as phosphoinositide 3-kinase (PI3K) to govern various pivotal cellular functions[11,12,13]. The ligands of many GPCRs have been identified, but it is still unknown the ligands of some GPCRs which are known as orphan receptors. Amino acids are ligands of some GPCRs including T1R1/T1R3 and GPRC6A, and regulate cellular processes in a positive feedback way through upregulating expression of these GPCRs[14,15,16]. It is still known little about other GPCRs sensing different amino acids.

Methionine (Met) is well known a sulfur-containing amino acid and one of the restrictive essential amino acids for animals and human being. Met is not only a substrate for protein synthesis, but also a key stimulus to regulate cell proliferation and various cellular metabolic processes[17]. Met can promote milk synthesis and proliferation of MECs through a multitude of signaling pathways, such as the SNAT2, PI3K, and GPR87 signaling pathway[8,18,19]. It remains elusive the exact GPCR capable of perceiving Met.

It has been reported that GPR183 is the oxysterol receptor, playing an important role in inflammation and immune response[20,21]. GPR183 participates in the progression of various diseases and has considerable potential as a pharmacological target[20,22]. Notably, GPR183 is

highly expressed in the small intestine of mice, and promotes lymphoid organ development[21]. Stimulation with GPR183 and its ligand oxysterol 7α,25-dihydroxycholesterol (7α,25-OHC) facilitated the intracellular proliferation of mycobacterium tuberculosis[23]. These reports point out that GPR183 undertakes multiple important roles in regulating cellular physiology, but it has not been reported the role of GPR183 in milk synthesis and amino acid sensing pathway.

Transcriptomic analysis can find new genes associated with milk synthesis in MECs and cell proliferation[24,25,26]. Furthermore, amino acids can stimulate expression of some GPCRs which can stimulate milk synthesis in MECs, and these GPCRs might be receptors of amino acids[8,16,19]. Thus, in this study, we employ transcriptome sequencing and gene function study approaches to uncover GPCRs which can sense Met in MECs.

Materials and methods

Collection of mouse mammary gland tissues

Mouse mammary gland tissue samples were collected, and animal experiments were performed according to the Regulations on Animal Experimentation of Yangtze University. Briefly, 12 normally raised female ICR mice fed with maintenance diet were divided into 3 groups (n = 4 in each group): group 1: puberty, 8-week-old; group 2, on the 14th day of lactation, 11-week-old; group 3, on the 3rd day of dry period, 12-week-old. The dislocation of the spinal cord was used to kill these mice, and then tissues of these mammary glands were collected, and stored in a −80°C refrigerator.

Cell culture and treatment

HC11 cells were purchased from the Cell Repository/Stem Cell Repository of the Chinese Academy of Sciences (Shanghai, China). Cells were cultivated for successive passages in RPMI 1640 Medium (31800-022, Gibco, Grand Island, NY, USA), supplemented with 10% fetal bovine serum (FBS, PAN-Biotech, Adenbach, Bavaria, Germany), $NaHCO_3$, sodium pyruvate (Gibco), GlutaMAX-1 (35050-61, Gibco), as well as 100 U/mL penicillin and 0.1 mg/mL streptomycin. These cultured cells were subsequently employed for subsequent experiments. For Met treatment, the original culture medium was replaced with OPTI-MEM I (31985-070, Gibco) free of FBS, upon the cell growth density reaching 40% in a 6-well or 24-well plate. Cells were then starved for 12 h, and next treated with Met at different concentrations at 37 °C for 24 h.

Construction of cDNA library and RNA-sequencing

Cells in a 6-well plate were treated with Met (0.6 mM) (3 blank samples and 3 Met-treated samples) for 24 h. As previously reported, this concentration of Met can effectively stimulate mTOR activation and milk synthesis in MECs[18]. Then within a few minutes a portion of these cells was swiftly placed in cryopreservation tubes containing the RNA Stabilization Reagent for Animal Tissue (R0118, Beyotime, Beijing, China), followed by rapid freezing in liquid nitrogen. The remaining cells were designated for Western blotting prior to subsequent sequencing endeavors. The processed cell samples were preserved on dry ice and sent to APTBIO (Shanghai, China) for transcriptome sequencing.

To construct the cDNA Library, total RNA was extracted from the cellular samples using TRIZOL reagent. The absorbance ratio of A260/A280 in the RNA samples was assessed using a Nanodrop ND-2000 instrument (Thermo, Waltham, MA, USA), while the RNA's integrity was evaluated through determination of the RNA Integrity Number (RIN) using the Agilent Bioanalyzer 4150 system (Agilent, Santa Clara, CA, USA). Paired-end libraries were prepared according to the instructions of the ABclonal mRNA-seq Library Preparation Kit (ABclonal, Wuhan, China). The library quality was assessed using the Agilent Bioanalyzer 4150. Lastly, the NovaSeq 6000 sequencing platform was employed with paired-end 150 base pair read length for the sequencing process.

Bioinformatics analysis

The data generated from the Illumina platform were utilized for bioinformatics analysis. The raw data were processed using a Perl script to remove adapter sequences and filter out reads with low quality (base quality value less than 20) as well as reads containing more than 5 undetermined bases. The resulting set of clean reads was employed for subsequent analyses. The HISAT2 software was utilized to align the clean reads with the reference genome, thereby the mapped reads were obtained for subsequent analysis.

DEGs selection and functional enrichment analysis

The differentially expressed genes (DEGs) were analyzed using DESeq2, with the filtering criteria set at log2FoldChange > 1.0 and Padj < 0.05 for upregulated DEGs and log2FoldChange < -1 and Padj < 0.05 for downregulated DEGs. The P values were adjusted to Padj using the Bonferroni correction method. GO and KEGG enrichment analyses were performed on upregulated or downregulated DEGs separately to elucidate the functional enrichment patterns of these genes using the R package "cluster Profiler".

RT-qPCR

Total RNA from HC11 cells was extracted using the Animal RNA Isolation Kit with Spin Column (R0026, Beyotime). RNA was reverse transcribed into cDNA using the BeyoRT II First Strand cDNA Synthesis Kit (RNase H minus) (D7168S, Beyotime). Quantitative real-time polymerase chain reaction (RT-qPCR) was carried out using the BeyoFast SYBR Green qPCR Mix (D7260, Beyotime) on the CFX96 Touch RT-PCR System (Bio-Rad, Hercules, CA, USA). For validation of the RNA-seq results, a total of 9 GPCRs with a log2FoldChange > 1.0 were selected. All primers were designed using Primer5 software for the 9 target genes and the reference gene (Table S1). *β-actin* mRNA was used as the reference, and normal cultured cells (cells not treated with Met) were used as the blank samples. RT-qPCR results were calculated using the $2^{-\Delta\Delta CT}$ method.

Transfection and screening of GPR183 siRNA

The GPR183 gene coding sequence was gained by employing the NCBI database. Three siRNAs fragments specific for different regions of GPR183 mRNA and a negative control siRNA (NC) were designed and made by GenePharma (Suzhou, China) (Table S2). Following a 24 h transfection period using GP-transfect-Mate (GenePharma), transfected cells were harvested for Western blotting to select the siRNA that had the best transfection efficiency. The most efficacious GPR183 siRNA sequences were: sense: 5'-GCUGGCCUUGGUUGUCAUUTT-3', antisense: 5'-AAUGACAACCAAGGCCAGCTT-3'.

Construction of GPR183 overexpression vector

The CRISPR/dCas9 gene editing technology was employed to activate GPR183 gene. dCas9 (dead Cas9) is a mutant of Cas9 protein, which is produced by the simultaneous mutation of the RuvC1 and HNH nuclease active regions of Cas9. Its cleavage enzyme activity is lost, and only the ability to be guided into the genome by gRNA is retained. Briefly, cells were co-transfected with the pSPgRNA vector (#47108, Addgene, Middlesex, UK) harboring specific single-guide RNA (sgRNA) sequence and the CRISPR/dCas9 vector SP-dCas9-VPR (hereinafter referred to as VPR) (#63798, Addgene) to achieve the activation of the GPR183 gene. The VPR plasmid contains three transcription factor binding domains (VP64, p65 and Rta) arranged in sequence at the dCas9 C-terminus. Thus VPR and pSPgRNA co-tranfection is able to achieve strong target gene transcriptional activation[27]. To design sgRNA, the promoter sequence of GPR183 was retrieved from www.ncbi.nlm.nih.gov, then 4 distinct sgRNA fragments were designed on www.zlab.bio.These sgRNAs were synthesized by BGI Genomics (Shenzhen, China). The DNA sequences of these 4 segments

were as follows: sgRNA-1: 5'-CACCAGAATGGAGTTAGCTAAGCTGGG-3'; sgRNA-2: 5'-CACCGAAAAAGGCACCACCATAAAAGG-3'; sgRNA-3: 5'-CACCTATGTGAGGTTAACTGATCACGG-3'; sgRNA-4: 5'-CACCAAAAGCACGTAGCATATGTGAGG-3'. To construct the recombinant pSPgRNA vector, the pSPgRNA vector was cleaved using the Bbs I restriction endonuclease, and ligated with the annealed oligonucleotides of the 4 sgRNAs. These 4 recombinant plasmids were named as: pSPgRNA-1, pSPgRNA-2, pSPgRNA-3, and pSPgRNA-4.

Transfection and selection of the GPR183 overexpression vector

Two μg recombinant pSPgRNA plasmid and 2 μg VPR plasmid were mixed with 196 μL of OPTI-MEM I to form solution A. Six μL GP-transfect-mate transfection reagent was added into 194 μL of OPTI-MEM I to create solution B. Then solution A and B were blended to form the DNA-lipid complex solution, which was then added into the cell culture medium. Following 48 h transfection, cells were collected for Western blotting to select the optimal GPR183 overexpression vector.

Western blotting

Cell samples were subjected to protein extraction using RIPA enzymatic degradation. Protein samples (20 μg/lane) were segregated on an 8% SDS polyacrylamide gel, subsequently translocated onto nitrocellulose membranes. These membranes were immersed in a 5% skimmed milk sealing solution at 37 ℃ for 1.5 h. Then they were incubated with the primary antibody at 4 ℃ for 12 h. Primary antibodies used were as follow: GPR183 (12377-1-AP, Proteintech, 1:800), β-actin (66009-1-Ig, Proteintech, 1:5000), β-casein (bs-10032R, Bioss, Beijing, China, 1:500), mTOR (66888-1-Ig, Proteintech, 1:5000), p-mTOR (67778-1-Ig, Proteintech, 1:2000), AKT (60203-2-Ig, Proteintech, 1:5000) and p-AKT (29163-1-AP, Proteintech, 1:1000). Subsequently, these membranes were incubated with horseradish peroxidase-conjugated goat anti-rabbit secondary antibody (ZB-2301, ZSGB-BIO, Beijing, China, 1:2000) or goat anti-mouse secondary antibody (ZA-2305, ZSGB-BIO, 1:2000) at 37 ℃ for 1 h. Finally, protein bands were detected by a chemiluminescence gel imaging system (JS-1070, Peiqing, Shanghai, China). Quantification of protein levels was accomplished using the ImageJ software.

CCK-8 assay

Cell proliferation level was assessed using the CCK-8 assay. Briefly, cells were mixed evenly and placed in a 96-well plate (~5 × 10^3 cells/well, 100 μL). Following further treatments, each well was supplemented with 10 μL of CCK-8 reagent (C0038, Beyotime). Then the plate was maintained at 37 ℃ for 2 h. Finally, absorbance measurements were taken

at 450 nm using a microplate reader (WD-2102B, Liuyi, Beijing, China).

EdU assay

EdU assay was employed to assess cell proliferation capability using the BeyoClick EdU-488 Cell Proliferation Detection Kit (C0071s, Beyotime), according to the manufacturer's guidelines. The fluorescence in cells was observed using a fluorescence inverted microscope (ICX41, Sunny, Ningbo, China).

TGs content detection

The content of triglycerides (TGs) in HC11 cells was quantitatively assessed using a TGs assay kit (E1013, Applygen, Beijing, China), according to the manufacturer's operational manual.

Observation of lipid droplet formation

Cells after treatments were fixed onto coverslips using a 4% paraformaldehyde solution. The hydrophobic fluorescence probe BODIPY (D3922, Invitrogen) was utilized at a concentration of 1 μg/mL to label lipid droplets. Subsequently, 4,6-diamidino-2-phenylindole (DAPI) (C1006, Beyotime) was employed to label nucleus. Lipid droplets in cells were observed under a fluorescence inverted microscope.

Statistical analysis

The experimental data represent the mean ± standard error of three (for cell experiments) or four (for mouse experiment) repeated experiments. Statistical software IBM SPSS (IBM, Armonk, New York, NY, USA) was used for statistical analysis. Analysis of variance (ANOVA) or Student's t-test was applied to determine the difference among the mean values. Different lowercase letters denote significant differences ($p < 0.05$); *, $p < 0.05$.

Results

DEGs in cells treated with Met

Western blotting was performed to validate the effectiveness of Met (0.6 mM) on cells, prior to conducting transcriptome sequencing. The effectiveness of Met was confirmed by the observation that Met significantly increased mTOR phosphorylation (Figure S1A,B). For RNA-seq, the RNA quality of samples was firstly assessed to validate whether they met sequencing requirements. The quality assessment results of RNA-seq showed that the Raw reads in the library of the blank group ranged from 40864078 to 65108516, with Clean reads spanning from 40519526 to 65007162. The Raw reads in the library of Met-treated group ranged from 42218702 to 70330244, and the Clean reads from 40896918 to 70223266 (Table S3). The filtration of data falled within a reasonable range. The base quality value Q20 (sequencing error rate P < 1/100) for the six samples was ≥ 96.34, and Q30 (sequencing error

rate P < 1/1000) was ≥ 91.06 (Table S3). The GC content was also within a reasonable range, indicating the absence of contamination in the cellular samples. The sequencing base error rate was a mere 0.05%. In the blank group, the proportion of total mapped reads to total clean reads ranged from 83.42% to 89.29%; and in the Met-treated group, it ranged from 82.18% to 92.78%. The unique mapped reads accounted for 72.75% to 83.78% and 71.58% to 83.94% of Total clean reads in the blank and Met-treated group, respectively (Table S4). From these above data, it is evident that the RNA-seq data possesses high quality and is suitable for subsequent analysis.

The RNA-seq data were analyzed using Illumina sequencing and DESeq2. The expression levels of each gene in various samples were computed as FPKM (expected number of fragments per kilobase of transcript sequence per millions base pairs sequenced) by using the featurecounts software. A padj value < 0.05 and an absolute log2FoldChange > 1 were used as the criteria for filtering DEGs, and a volcano plot of DEGs was generated. Cluster analysis of DEGs and the volcano plot showed substantial disparities in gene expression between cell samples with and without Met treatment (Figure 1, Figure S2). From these, 129 genes were screened out. Among these genes, 59 genes were upregulated, and 70 genes were downregulated. These DEGs might potentially mediate the effects of Met on HC11 cells.

GO annotation of DEGs

Gene Ontology (GO) comprises three major structural domains: biological process, molecular function, and cellular component. The top 10 enriched functional terms were selected from each of these domains, sorted by P-value. Within the upregulated GO of the Met-treated group compared to the blank group, biologically significant enriched processes encompassed cell proliferation, nutrient transportation, metabolic byproducts and energy generation, as well as cell surface receptor activity; molecular functionalities encompassed NADH dehydrogenase activity, oxidoreduction-driven active transmembrane transporter activity, electron transfer activity, primary active transmembrane transporter activity, and glutamate receptor binding; and prominently enriched cellular components encompassed respirasome, inner mitochondrial membrane protein complex, respiratory chain complex I, NADH dehydrogenase complex, etc. (Figure S3A).

The GO of downregulated expression primarily encompassed biological processes included adult behavior, developmental maturation, neuronal ion channel clustering, calcium ion-regulated exocytosis of neurotransmitters, and nervous system development; notably enriched molecular functionalities encompassed metal ion transmembrane transporter activity, protein C-terminus binding, transmembrane transporter activity, and more (Figure S3B); and

mainly involved cellular components included presynapse, axon, neuron projection terminus, and synaptic membrane.

KEGG enrichment analysis of DEGs

The Kyoto Encyclopedia of Genes and Genomes (KEGG) database in conjunction with the Fisher's exact test were used to analyze the enrichment levels of signal pathways among genes in the Met-treated group compared to the blank group.

Significantly enriched signal pathways among the upregulated genes comprised prion disease, oxidative phosphorylation, retrograde endocannabinoid signaling, endocrine resistance, breast cancer, mTOR signaling pathway, proteoglycans in cancer, etc. (Figure 2A).

The significantly enriched signal pathways among the downregulated genes encompassed pancreatic secretion, protein digestion and absorption, glutamatergic synapse, taurine and hypotaurine metabolism, phospholipase D signaling pathway, butanoate metabolism, cAMP signaling pathway, beta-alanine metabolism, and alanine, aspartate, and glutamate metabolism, etc. (Figure 2B).

Candidate GPCRs selection and RT-qPCR validation

From the RNA-seq data (upregulated DEGs) and GO and KEGG analysis, and further compared with the Mouse Genome Informatics (MGI) database, an international database resource for the laboratory mouse, 9 GPCRs were selected: Gpr183, Gpr171, Gpr31b, Gpr141, Gpr21, Gprc5d, Mrgprf, Mrgprb3 and Mrgprx2. RT-qPCR analysis validated that most of these GPCR RNA-seq results had high reliability (Figure 3).

GPR183 is highly expressed in mouse mammary gland tissue during the lactation stage

By analyzing previous literature on these GPCRs, GPR183 was further selected to analyze its role in Met-stimulated milk synthesis in HC11 cells. We firstly observed the expression of GPR183 by Western blotting analysis in mouse mammary gland tissues during puberty, lactation, and involution stages. GPR183 protein was much more highly expressed in tissues during lactation stage, compared with the other two stages (Figure 4A,B). These data suggest that GPR183 might play a pivotal regulatory role in milk synthesis in mammary gland.

GPR183 positively regulates milk protein and fat synthesis in HC11 cells and cell proliferation

Gene function analysis was performed to determine the role of GPR183 in HC11 cells. GPR183 was knocked down through transfection of GPR183 siRNA into HC11 cells. Three GPR183 siRNAs were separately introduced into HC11 cells, and the third siRNA exhibited the most robust interference efficacy, which was chosen for subsequent experiments (Figure 5A,B). GPR183 knockdown significantly decreased β-casein level (Figure 5C,D) and content

of TGs (Figure 5E) and formation of lipid droplets (Figure 5F) in cells , and also reduced cell number (Figure 5G) and proliferation ability (Figure 5H).

GPR183 overexpression was performed using the CRISPR/dCas9 technology. Western blotting detected that the first pSPgRNA among the 4 recombinant plasmids yielded the most potent overexpression effect (Figure 6A,B), which was selected for subsequent experiments. GPR183 overexpression significantly upregulated β-casein level (Figure 6C,D) and content of TGs (Figure 6E) and formation of lipid droplets (Figure 6F) in cells , and also increased cell number (Figure 6G) and proliferation ability (Figure 6H). In summary, these above data demonstrate that GPR183 is a positive regulator of milk protein and fat synthesis in HC11 cells and cell proliferation.

GPR183 positively regulates mTOR phosphorylation and mRNA expression

The effects of GPR183 on mTOR activation were further observed. GPR183 knockdown (Figure 7A,B) significantly reduced mTOR phosphorylation (Figure 7A,C), whereas GPR183 overexpression (Figure 7D,E) had an opposite effect (Figure 7D,F). RT-qPCR analysis detected a significant decrease in mTOR mRNA expression upon GPR183 knockdown (Figure 7G). Conversely, GPR183 activation led to a markedly increase in mTOR mRNA expression (Figure 7H). These data demonstrate that GPR183 is a positive regulator of mTOR mRNA expression and protein activation.

Met stimulates GPR183 expression in a dose dependent manner

We further observed the influence of Met on HC11 cells. Cells were treated with Met (0, 0.2, 0.4, 0.6, 0.8, and 1.0 mM) for 24 h. GPR183 protein expression levels were gradually increased with increasing concentrations of Met (Figure 8A,B). The peak expression was attained at a concentration of 0.6 mM, followed by a subsequent decline. Expectedly, the phosphorylation level of mTOR also had the same trend (Figure 8A,C). These data suggest that, in responding to Met stimulation, the expression level of GPR183 can be changed to exert its regulatory role in sensing Met to activate mTOR.

GPR183 mediates Met stimulation on milk protein and fat synthesis, cell proliferation and mTOR activation

We next determined the effects of GPR183 in Met function on HC11 cells. GPR183 knockdown blocked the increase by Met of β-casein level (Figure 9A,B) and content of TGs (Figure 9C) and formation of lipid droplets (Figure 9D) in cells , and also cell number (Figure 9E) and proliferation ability (Figure 9F). GPR183 knockdown (Figure 10A,B) also diminished the stimulation of Met on mTOR phosphorylation (Figure 10A,C) and mRNA expression (Figure 10D). Collectively, these above data demonstrate that GPR183 is a key

mediator for Met to stimulate mTOR phosphorylation, and milk protein and fat synthesis and cell proliferation.

GPR183 stimulates mTOR phosphorylation and mRNA expression in a PI3K dependent manner

Since many GPCRs can function through the PI3K signaling, we further determined whether GPR183 can function in a PI3K dependent manner. PI3K inhibition by LY294002 treatment almost entirely abrogated the induction of GPR183 overexpression (Figure 11A,B) on mTOR (Figure 11A,C) and AKT phosphorylation (Figure 11A,D).The effect of LY294002 on PI3K inhibition was confirmed by the observation of AKT phosphorylation, which is a direct substrate of PI3K (Figure 11A,D). PI3K inhibition also abrogated the induction of GPR183 overexpression on *mTOR* mRNA expression (Figure 11E). We noted that PI3K inhibition also markedly decreased GPR183 expression, indicating that there might be a positive feedback mechanism in GPR183 signaling to PI3K activation. Collectively, these data suggest that GPR183 might regulate mTOR phosphorylation and mRNA expression in a PI3K dependent manner.

Discussion

GPCRs represent the largest family of cell surface receptors. Though it has been reported that a few GPCRs can sense several different amino acids, the GPCRs sensing Met remains elusive. In this study, DEG analysis of RNA-seq libraries showed that 129 genes were differently expressed between blank and Met-treated HC11 cells, in which 59 genes were upregulated in cells treated with Met, while 70 genes were downregulated. From these, we further identified a subset of upregulated GPCRs, encompassing 9 members: Gpr183, Gpr171, Gpr31b, Gpr141, Gpr21, Gprc5d, Mrgprf, Mrgprb3 and Mrgprx2, and most of them were validated by RT-qPCR analysis. We further showed that GPR183 was highly expressed in mouse mammary tissue during lactation stage. Gene function study demonstrates that GPR183 positively regulates mTOR phosphorylation and mRNA expression, milk protein and fat synthesis, and cell proliferation. Met can affect GPR183 expression in a dose dependent manner, and GPR183 mediates the impact of Met on mTOR phosphorylation and mRNA expression, milk protein and fat synthesis, and cell proliferation. GPR183 functions in a PI3K-dependent manner.

GPR183 is known as a chemotactic receptor, playing important role in B cell maturation, and its endogenous ligand is 7α,25-OHC[28]. GPR183 can produce hypersensitivity in the spinal cord through the MAPK and NF-κB signaling pathways[29]. Our experimental data uncover that GPR183 mediates Met signaling to mTOR activation and milk protein and fat

synthesis and cell proliferation. Though it has not been reported that GPR183 can participate in Met sensing, a few recent reports have pointed that GPR183 can regulate the mTOR signaling pathway, in support of our finding. GPR183 can mediate the induction of 7α,25-OHC on oxiapoptophagy of mouse fibroblast cells[30], and a recent report uncover that GPR183 functions through regulating the PI3K-mTOR signaling pathway[31]. Our experimental data suggest that GPR183 might be the receptor of Met, which is worth to be explored in future study.

Our experimental data validated that 0.6 mM Met is the optimal concentration of Met to influence β-casein synthesis and proliferation of mouse MECs, in agreement with previous reports[18,32]. At 0.6 mM concentration, Met has the best stimulatory effect on expression of GPR183, which can mediate Met induction of mTOR activation. At this concentration, Met can also stimulate expression of the typical amino acid transporters such as SNAT2, which can transport Met into cells for its utilization, to activate mTOR[18]. It is still unknown whether GPCRs is a competitor of Met transporters for mTOR activation, or they may collaborate to activate mTOR under Met stimulation.

It is still largely unknown the exact GPCR sensing Met. Several GPCRs have been reported the receptors of amino acids. Previous reports have pointed out that the GPCR T1R1-T1R3, a class C GPCR, can sense L-amino acids such as Phe, Leu, and Glu, and T1R1-T1R3 partly mediates amino acid signaling to mTOR activation[33,34,35]. GPRC6A can be activated by multiple ligands including basic amino acids such as Lys[15,36].We have previously shown that Met and taurine can stimulate mTOR phosphorylation and milk synthesis in MECs in a GPR87 dependent manner[19,37], but the detailed mechanism is still unknown. In this study, we demonstrate that Met stimulates milk protein and fat synthesis and cell proliferation in a GPR183 dependent manner. In future study, to uncover whether GPR183 is a GPCR sensing Met, we need to determine the N-terminal binding site for Met in GPR183 protein and which G protein transmit the signal of GPR183 to activate the PI3K-mTOR signaling.

We showed that GPR183 mediated Met stimulation on mTOR mRNA expression and protein phosphorylation. This observation is in consistent with previous reports. It has been well established that amino acids can directly activate mTOR in the cytoplasm[38]. We have previously shown that the activation of mTOR by amino acids such as Met, Leu, and taurine also depends on its transcriptional activation, which will provide sustained mTOR protein for phosphorylation[39,40,41,42]. From these previous reports and our experimental data, we conclude that Met and GPR183 can promote mTOR mRNA expression and activation.

In summary, this study identifies a total of 129 DEGs in HC11 cells under Met stimulation. Furthermore, we elucidate that GPR183 is a positive regulator mediating Met stimulation on milk protein and fat synthesis and cell proliferation through activating the PI3K-mTOR signaling. Our findings would furnish novel theoretical underpinnings for the application of Met in milk production.

Supporting information

Figure S1-S3, and Table S1-S4.

Funding

This work was supported by grants from National Natural Science Foundation of China (No. 31671473).

Conflict of Interest Statement

The authors declare that they have no known competing financial interests or personal relationships that could have appeared to influence the work reported in this paper.

Acknowledgments

Yuwen Zhou: Perform experiments, collect and analyze data, and write manuscript. Ming Xu and Sihua Fan: Perform experiments. Minghui Zhang: Funding, Analyze data. Xuejun Gao: Design experiments, and write and review manuscript.

Data Availability Statement

The data that support the findings of this study are available from the corresponding author upon reasonable request.

ORCID

Yuwen Zhou: 0009-0001-3389-5256, Minghui Zhang: 0000-0002-8253-1379, Xuejun Gao: 0000-0002-8241-6346.

References

1. Truchet S, Honvo-Houéto E (2017) Physiology of milk secretion. *Best Pract Res Clin Endocrinol Metab* **31**, 367-384.

2. Herve L, Quesnel H, Lollivier V *et al.* (2016) Regulation of cell number in the mammary gland by controlling the exfoliation process in milk in ruminants. *J Dairy Sci* **99**, 854-863.

3. Boutinaud M, Guinard-Flamenta J, Jammes H (2004) The number and activity of mammary epithelial cells, determining factors for milk production. *Reprod Nutr Dev* **44**, 499-508.

4. Hannan FM, Elajnaf T, Vandenberg LN *et al.* (2023) Hormonal regulation of mammary gland development and lactation. *Nat Rev Endocrinol* **19**, 46-61.

5. Sabatini DM (2017) Twenty-five years of mTOR: Uncovering the link from nutrients to growth. *Proc Natl Acad Sci U S A* **114**, 11818-11825.

6. Wullschleger S, Loewith R, Hall MN *et al.* (2006) TOR signaling in growth and metabolism. *Cell* **124**, 471-484.

7. Szwed A, Kim E, Jacinto E *et al.* (2021) Regulation and metabolic functions of mTORC1 and mTORC2. *Physiol Rev* **101**, 1371-1426.

8. Han M, Zhang M *et al.* (2023) The regulatory mechanism of amino acids on milk protein and fat synthesis in mammary epithelial cells: a mini review. *Anim Biotechnol* **34**, 402-412.

9. Kim JE, Lee HG *et al.* (2021) Amino acids supplementation for the milk and milk protein production of dairy cows. *Animals (Basel)* **11**, 2118.

10. Jakubík J, El-Fakahany EE *et al.* (2021) Allosteric modulation of GPCRs of Class A by cholesterol. *Int J Mol Sci* **22**, 1953.

11. Seyedabadi M, Ghahremani MH, Albert PR *et al.* (2019) Biased signaling of G protein coupled receptors (GPCRs): Molecular determinants of GPCR/transducer selectivity and therapeutic potential. *Pharmacol Ther* **200**, 148-178.

12. Wang J, Hua T, Liu ZJ *et al.* (2020) Structural features of activated GPCR signaling complexes. *Curr Opin Struct Biol* **63**, 82-89.

13. Carnero A (2009) Novel inhibitors of the PI3K family. *Expert Opin Investig Drugs* **18**, 1265-1277.

14. Zheng L, Zhang W, Zhou Y *et al.* (2016) Recent advances in understanding amino acid sensing mechanisms that regulate mTORC1. *Int J Mol Sci* **17**, 1636.

15. Pi M, Nishimoto SK, Quarles LD *et al.* (2016) GPRC6A: Jack of all metabolism (or master of none). *Mol Metab* **6**, 185-193.

16. Li X, Li P, Wang L *et al.* (2019) Lysine enhances the stimulation of fatty acids on milk fat synthesis via the GPRC6A-PI3K-FABP5 signaling in bovine mammary epithelial cells. *J Agric Food Chem* **67**, 7005-7015.

17. Mladenović D, Radosavljević T, Hrnčić D *et al.* (2019) The effects of dietary methionine restriction on the function and metabolic reprogramming in the liver and brain-implications for longevity. *Rev Neurosci* **30**, 581-593.

18. Qi H, Meng C, Jin X *et al.* (2018) Methionine promotes milk protein and fat synthesis and cell proliferation via the SNAT2-PI3K signaling pathway in bovine mammary epithelial cells. *J Agric Food Chem* **66**, 11027-11033.

19. Luo C, Yu M, Li S *et al.* (2020) Methionine stimulates GlyRS phosphorylation via the GPR87-CDC42/Rac1-MAP3K10 signaling pathway. *Biochem Biophys Res Commun* **523**, 847-852.

20. Misselwitz B, Wyss A, Raselli T *et al.* (2021) The oxysterol receptor GPR183 in inflammatory bowel diseases. *Br J Pharmacol* **178**, 3140-3156.

21. Emgård J, Kammoun H, García-Cassani B *et al.* (2018) Oxysterol sensing through the receptor GPR183 promotes the lymphoid-tissue-inducing function of innate lymphoid cells and colonic inflammation. *Immunity* **48**, 120-132.e8.

22. Frascoli M, Ferraj E, Miu B *et al.* (2023) Skin γδ T cell inflammatory responses are hardwired in the thymus by oxysterol sensing via GPR183 and calibrated by dietary cholesterol. *Immunity* **56,** 562-575.e6.

23. Tang J, Shi Y, Zhan L *et al.* (2020) Downregulation of GPR183 on infection restricts the early infection and intracellular replication of mycobacterium tuberculosis in macrophage. *Microb Pathog* **145**, 104234.

24. Finucane KA, McFadden TB, Bond JP *et al.* (2008) Onset of lactation in the bovine mammary gland: gene expression profiling indicates a strong inhibition of gene expression in cell proliferation. *Funct Integr Genomics* **8**, 251-264.

25. Sigl T, Meyer HH, Wiedemann S (2014) Gene expression analysis of protein synthesis pathways in bovine mammary epithelial cells purified from milk during lactation and short-term restricted feeding. *J Anim Physiol Anim Nutr (Berl)* **98**, 84-95.

26. Saeki K, Chang G, Kanaya N *et al.* (2021) Mammary cell gene expression atlas links epithelial cell remodeling events to breast carcinogenesis. *Commun Biol* **4**, 660.

27. Chavez A, Scheiman J, Vora S *et al.* (2015) Highly efficient Cas9-mediated transcriptional programming. *Nat Methods* **12**, 326-328.

28. Braden K, Giancotti LA, Chen Z *et al.* (2020) GPR183-oxysterol axis in spinal cord contributes to neuropathic pain. *J Pharmacol Exp Ther* **375**, 367-375.

29. Braden K, Campolo M, Li Y *et al.* (2022) Activation of GPR183 by 7α,25-Dihydroxycholesterol induces behavioral hypersensitivity through mitogen-activated protein kinase and nuclear factor-κB. *J Pharmacol Exp Ther* **383**, 172-181.

30. Kim JS, Lim H, Seo JY *et al.* (2022) GPR183 regulates 7α,25-dihydroxycholesterol-induced oxiapoptophagy in L929 mouse fibroblast cell. *Molecules* **27**, 4798.

31. Seo JY, Kim TH, Kang KR *et al.* (2023) 7α,25-Dihydroxycholesterol-induced oxiapoptophagic chondrocyte death via the modulation of p53-Akt-mTOR axis in osteoarthritis pathogenesis. *Mol Cells* **46**, 245-255.

32. Lin G, Qi H, Guo X *et al.* (2023) ARID1B blocks methionine-stimulated mTOR activation to inhibit milk fat and protein synthesis in and proliferation of mouse mammary epithelial cells. *J Nutr Biochem* **114**, 109274.

33. Daly K, Al-Rammahi M, Moran A *et al.* (2013) Sensing of amino acids by the gut-expressed taste receptor T1R1-T1R3 stimulates CCK secretion. *Am J Physiol Gastrointest Liver Physiol* **304**, G271-282.

34. Wang Y, Liu J, Wu H *et al.* (2017) Amino acids regulate mTOR pathway and milk protein synthesis in a mouse mammary epithelial cell line is partly mediated by T1R1/T1R3. *Eur J Nutr* **56**, 2467-2474.

35. Wauson EM, Zaganjor E, Cobb *et al.* (2013) Amino acid regulation of autophagy through the GPCR TAS1R1-TAS1R3. *Autophagy* **9**, 418-419.

36. He Y, Su J, Gao H *et al.* (2022) GPRC6A mediates glucose and amino acid homeostasis in mice. *Metabolites* **12**, 740.

37. Yu M, Wang Y, Wang Z *et al.* (2019) Taurine promotes milk synthesis via the GPR87-PI3K-SETD1A signaling in BMECs. *J Agric Food Chem* **67**, 1927-1936.

38. Wolfson RL, Sabatini DM (2017) The dawn of the age of amino acid sensors for the mTORC1 Pathway. *Cell Metab* **26**, 301-309.

39. Ke C, Zhao S, Wang L *et al.* (2023) Chromatin remodeler BRM is a key mediator of leucine-stimulated mTOR gene transcription in mouse mammary epithelial cells. *Biochem Biophys Res Commun* **643**, 88-95.

40. Qi H, Wang L, Zhang M *et al.* (2022) Methionine and leucine induce ARID1A degradation to promote mTOR expression and milk synthesis in mammary epithelial cells. *J Nutr Biochem* **101**, 108924.

41. Xu M, Zhou Y, Fan S *et al.* (2023) Cul5 mediates taurine-stimulated mTOR mRNA expression and proliferation of mouse mammary epithelial cells. *Amino Acids* **55**, 243-252.

42. Huo N, Yu M, Li X *et al.* (2019) PURB is a positive regulator of amino acid-induced milk synthesis in bovine mammary epithelial cells. *J Cell Physiol* **234**, 6992-7003.

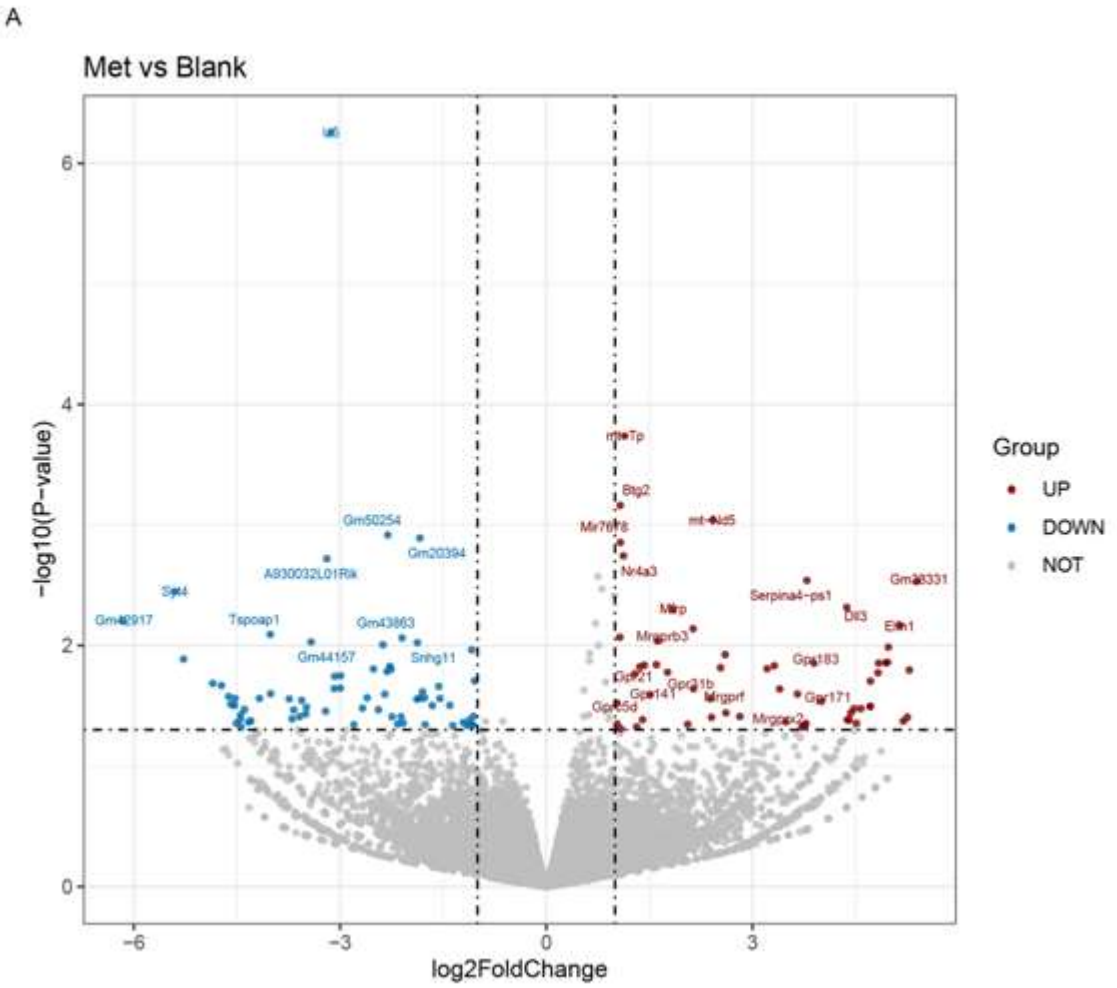

Figure 1. Analysis of DEGs between the blank and Met-treated group

Volcano plot of DEGs between the blank group and Met (0.6 mM) treatment group. The abscissa represented the change of gene expression multiple, and the ordinate indicated the significance of gene expression differences. Blue dot indicated down-regulated DEGs, red dot indicated up-regulated DEGs, and gray dot indicated genes without differential expression.

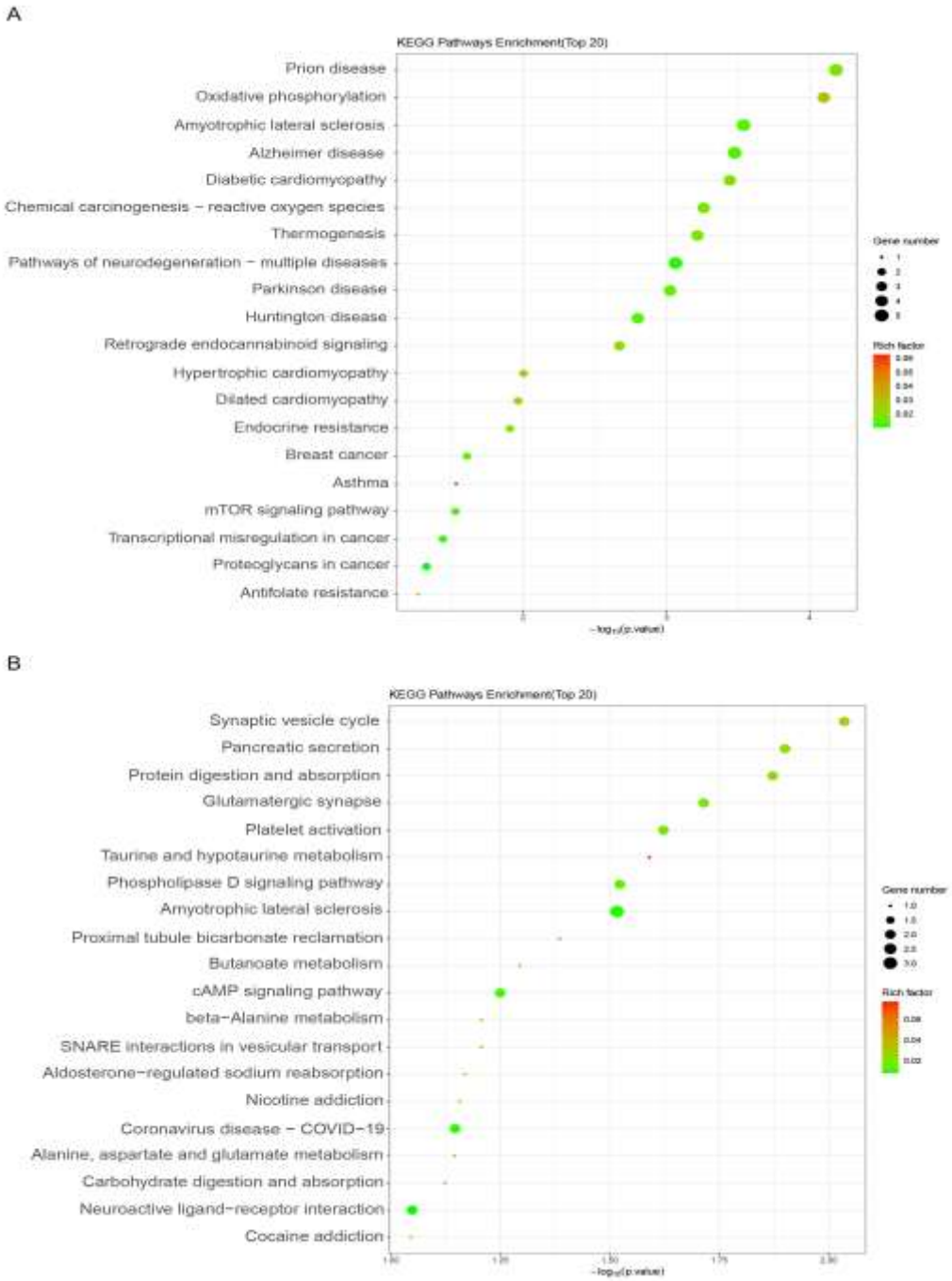

Figure 2. KEGG enrichment map of DEGs between the blank and Met-treated group

(A and B) KEGG enrichment plot of DEGs of upregulated (A) and downregulated (B) genes between the blank and Met (0.6 mM)-treated HC11 cells. The ordinate represented the name of the signaling pathway, and the abscissa represented the P value of the signaling pathway. The color of the dot represented the size of the rich factor. The size of the dot represented the number of differential genes contained in the signaling pathway.

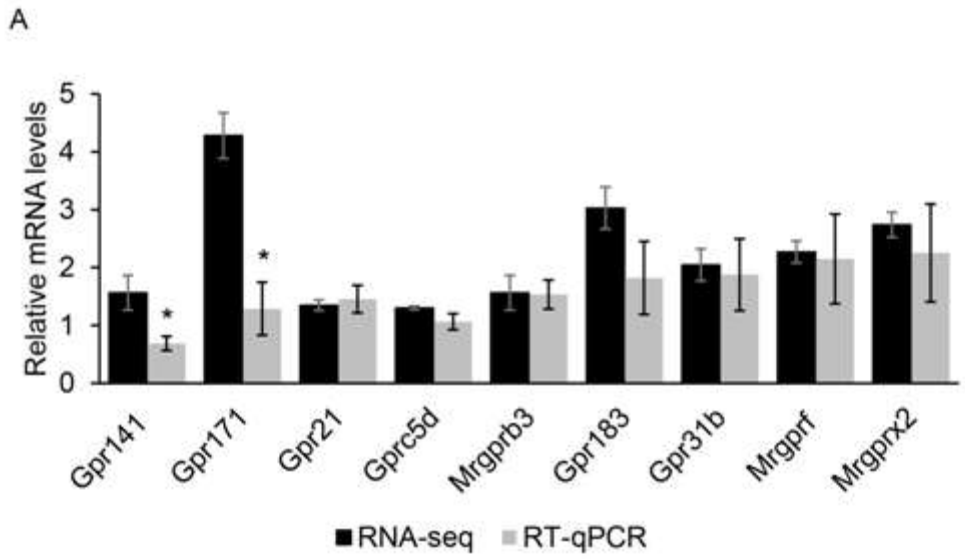

Figure 3. Comparison of RNA-seq and RT-qPCR results of 9 selected GPCRs

Comparison between RNA-seq and RT-qPCR results of 9 selected GPCRs. The relative mRNA level was the ratio of RNA-seq or RT-qPCR results of the Met treatment group to that of the control group. Data were the mean ± SE (n = 3). *, $p < 0.05$.

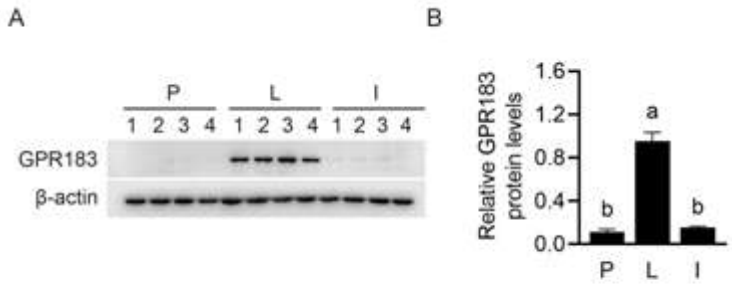

Figure 4. GPR183 expression in mouse mammary gland tissues during different stages.

(A) Western blotting analysis of GPR183 protein levels in mouse mammary gland tissues during puberty (P), lactation (L) and involution stages (I). (B) Quantification of GPR183 expression using ImageJ. Data were the mean ± SE (n = 4). Different letters marked above the values indicate significant differences ($p < 0.05$).

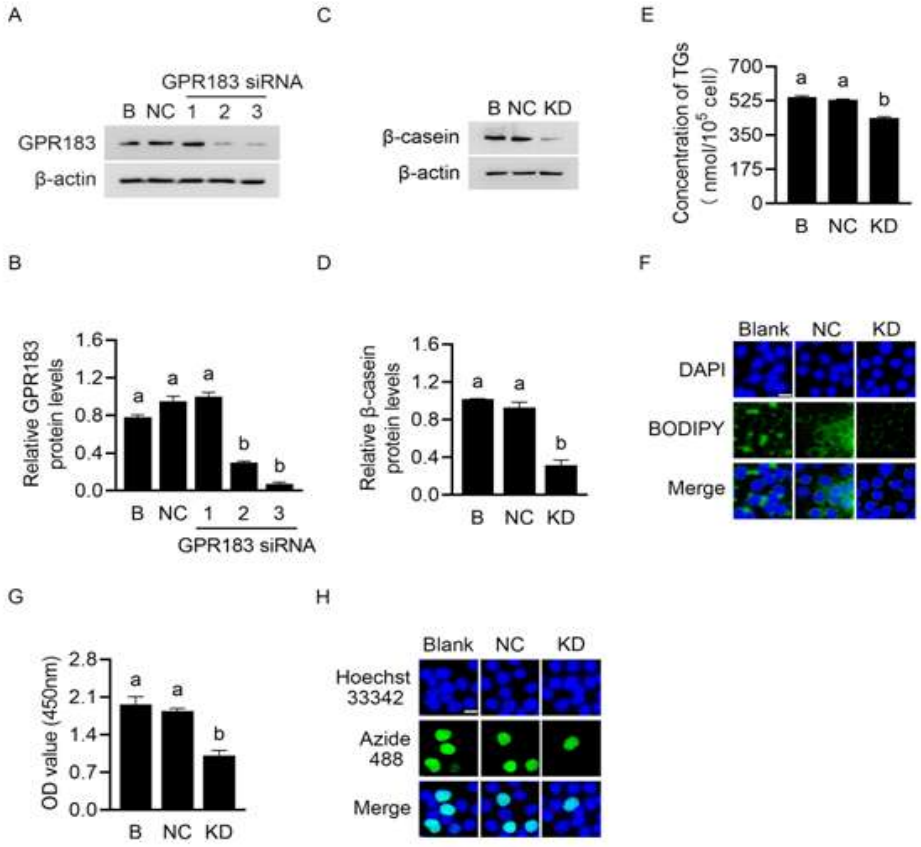

Figure 5. Effects of GPR183 knockdown on cell proliferation and milk protein and fat synthesis

(A) GPR183 protein levels in HC11 cells transfected with 3 different siRNAs were analyzed by Western blotting. 1, 2 and 3 represent 3 different siRNAs targeting GPR183. B, blank. (B) Quantification by ImageJ of GPR183/β-actin from Western blots in (A). (C) The protein level of β-casein in HC11 cells transfected with GPR183 siRNA3 was analyzed by Western blotting. Normal cultured HC11 cell was used as a blank control, and NC transfected cell was used as a negative control. (D) Quantification by ImageJ of β-casein/β-actin from Western blots in (C). (E) The content of TGs in cells was detected by a TG detection kit. (F) Lipid droplets in cells were observed using BODIPY staining. Lipid droplets labeled with BODIPY, green; nuclei labeled with DAPI, blue. Scale bar = 15 μm. (G) Cell number was determined using a CCK-8 detection kit. (H) Cell proliferation ability was determined using an EdU-488 detection kit. Azide 488 labeled proliferating cells, green; and Hoechst 33342 labeled nuclei, blue. Scale bar = 15 μm. Data were the mean ± SE (n = 3). Different letters marked above values indicate significant differences ($p < 0.05$).

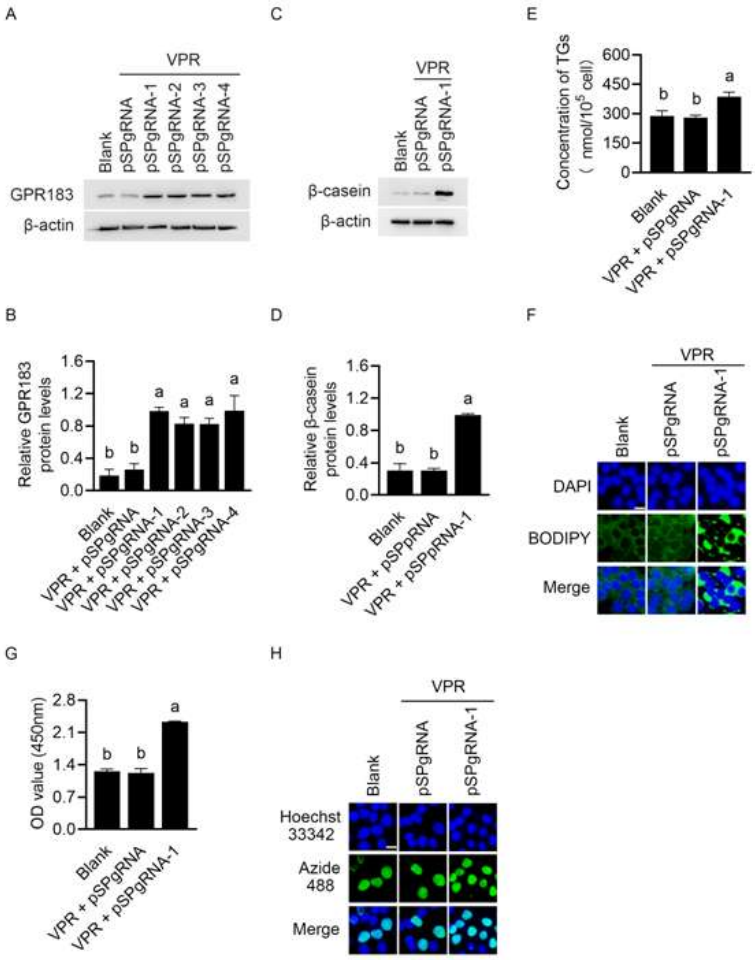

Figure 6. Effects of GPR183 overexpression on cell proliferation and milk protein and fat synthesis

(A) GPR183 protein levels in cells co-transfected with VPR and four different recombinant pSPgRNA vectors were detected by Western blotting. pSPgRNA-1, pSPgRNA-2, pSPgRNA-3 and pSPgRNA-4: 4 different pSPgRNA vectors. (B) Quantification by ImageJ of GPR183/β-actin expression from Western blots in (A). (C) The protein levels of β-casein in HC11 cells co-transfected with VPR and pSPgRNA-1 were analyzed by Western blotting. Normal cultured HC11 cell was used as a blank control, and empty pSPgRNA and VPR transfected cell as negative control. (D) Quantification by ImageJ of β-casein/β-actin expression from Western blots in (C). (E) The content of TGs in cells was detected by a TG detection kit. (F) Lipid droplets in cells were observed using BODIPY staining. Lipid droplets labeled with BODIPY, green; nuclei labeled with DAPI, blue. Scale bar = 15 μm. (G) CCK-8 assay of number of cells transfected with pSPgRNA-1. (H) EdU-488 cell proliferation detection kit was used to detect cell proliferation ability. Azide 488 labeled proliferating cells, green; and Hoechst 33342 labeled nuclei, blue. Scale bar = 15 μm. Data were the mean ± SE (n = 3). Different letters marked above values indicate significant differences ($p < 0.05$).

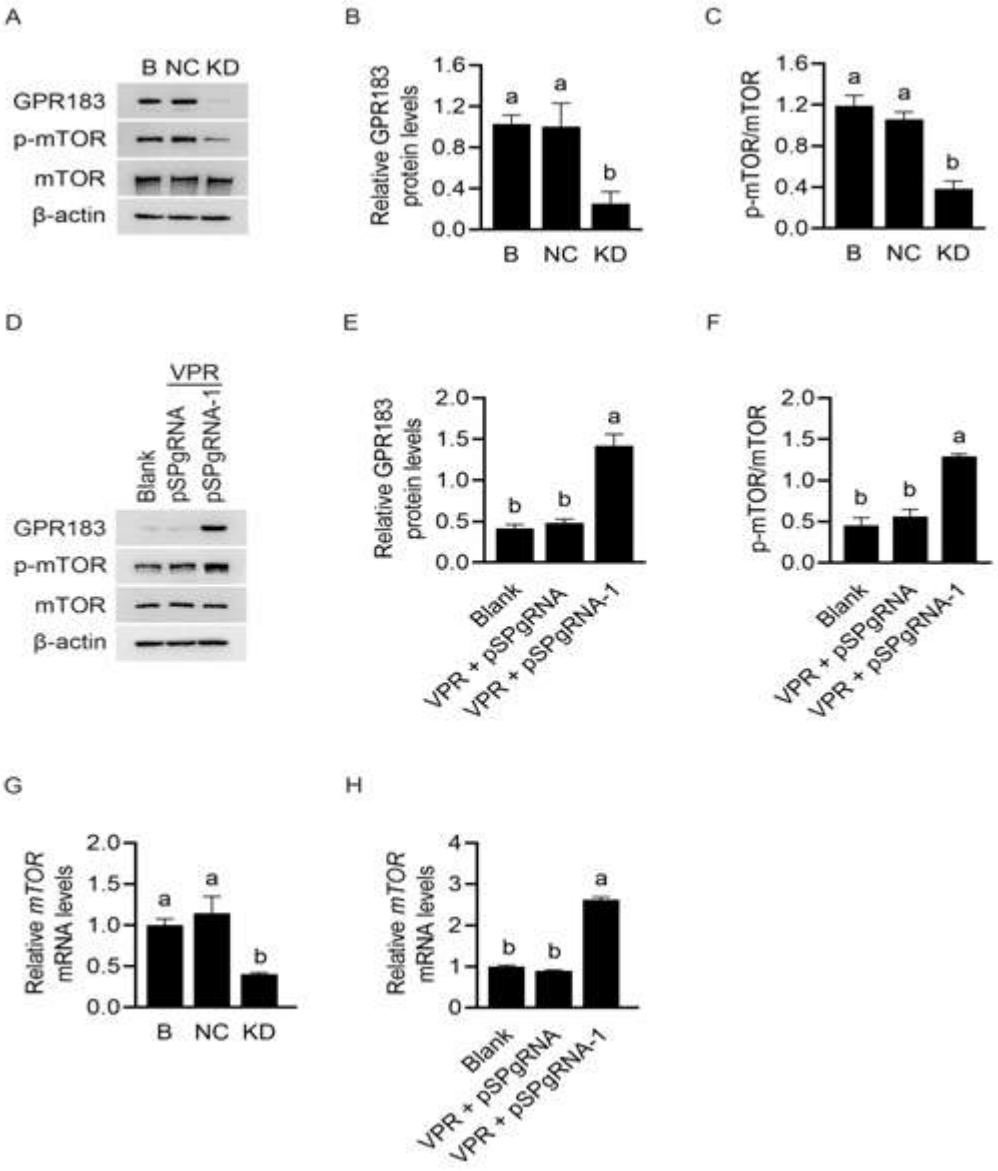

Figure 7. Effects of GPR183 on the mRNA expression and protein phosphorylation of mTOR

(A) Western blotting analysis of indicative protein levels in HC11 cells transfected with GPR183 siRNA-3. (B and C) Quantification by ImageJ of GPR183/β-actin (B) and p-mTOR/mTOR (C) from Western blots in (A). (D) Western blotting analysis of indicative protein levels in HC11 cells transfected with pSPgRNA-1. (E and F) Quantification by ImageJ of GPR183/β-actin (E) and p-mTOR/mTOR (F) from Western blots in (D). (G and H) RT-qPCR analysis of mRNA expression of *mTOR* in HC11 cells transfected with GPR183 siRNA-3 (G) or pSPgRNA-1 (H). Data were the mean ± SE (n = 3). Different letters marked above values indicate significant differences ($p < 0.05$).

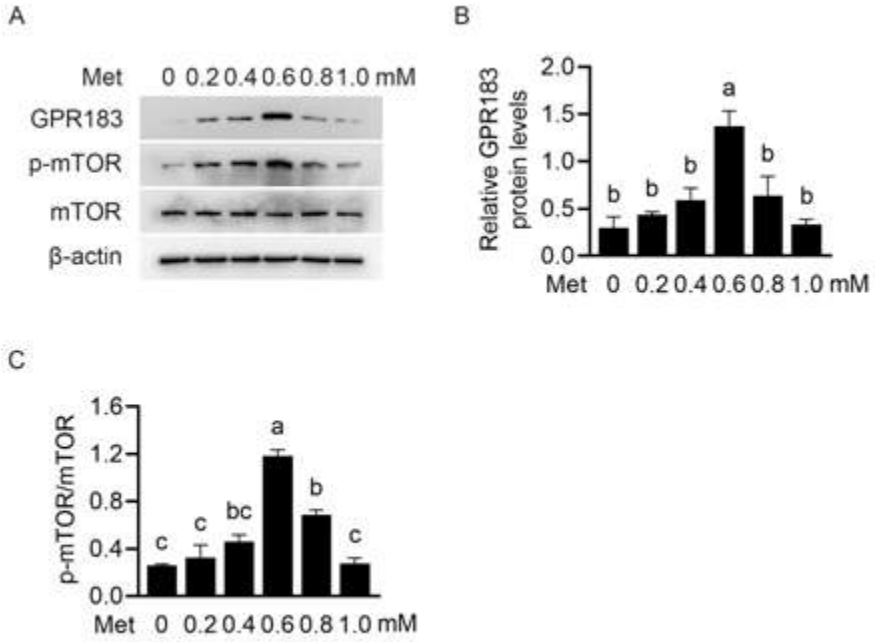

Figure 8. Effect of Met onGPR183 protein level in HC11 cells.

(A) HC11 cells were treated with different concentrations of Met (0, 0.2, 0.4, 0.6, 0.8, and 1.0 mM). Indicated protein levels were detected by Western blotting. (B and C) Quantification by ImageJ of GPR183/β-actin (B) and p-mTOR/mTOR (C) from Western blots in (A). Data were the mean ± SE (n = 3). Different letters marked above values indicate significant differences ($p < 0.05$).

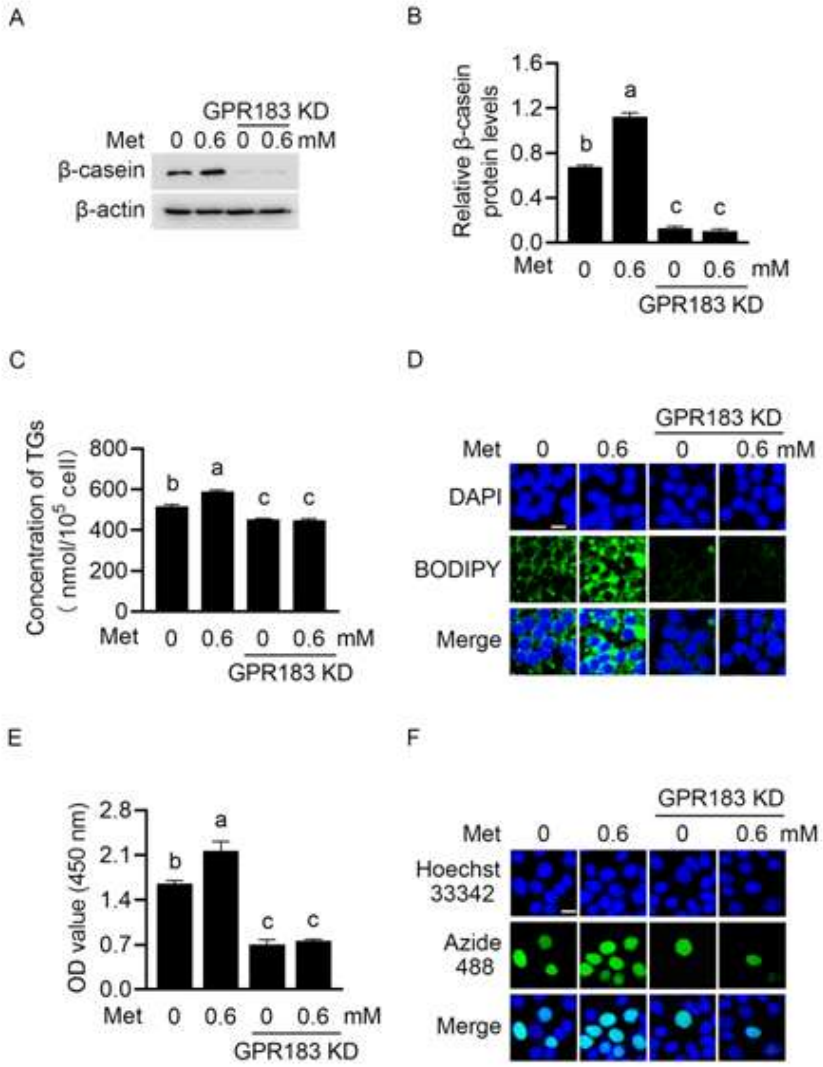

Figure 9. Effects of GPR183 on Met-stimulated cell proliferation and milk protein and fat synthesis.

(A) Western blotting analysis of β-casein protein levels in HC11 cells transfected with GPR183 siRNA-3 and treated with Met (0.6 mM) for 24 h. (B) Quantification by ImageJ of β-casein/β-actin from Western blots in (A). (C) The content of TGs in cells was detected by a TG detection kit. (D) Lipid droplets in cells were observed using BODIPY staining. Lipid droplets labeled with BODIPY, green; nuclei labeled with DAPI, blue. Scale bar = 15 μm. (E) CCK-8 assay of number of cells transfected with GPR183 siRNA-3 and stimulated by Met (0.6 mM) for 24 h. (F) An EdU-488 cell proliferation detection kit was used to detect cell proliferation ability. Azide 488 labeled proliferating cells, green; and Hoechst 33342 labeled nuclei, blue. Scale bar = 15 μm. Data were the mean ± SE (n = 3). Different letters marked above values indicate significant differences ($p < 0.05$).

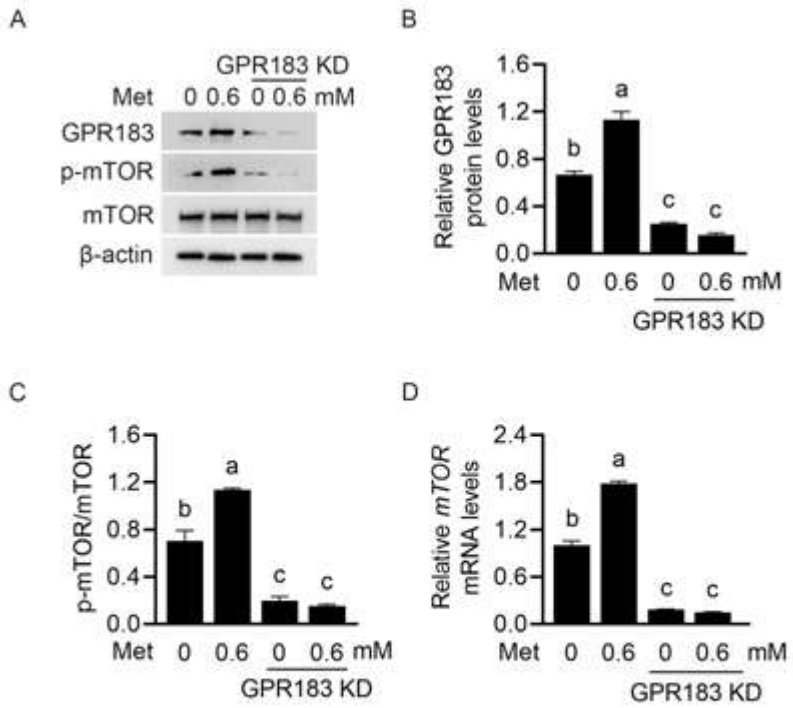

Figure 10. Effects of GPR183 on Met-stimulated mTOR mRNA expression and protein phosphorylation.

(A) Cells were treated as in Figure 9A. Indicated protein levels were detected by Western blotting. (B and C) Quantification by ImageJ of GPR183/β-actin (B) and p-mTOR/mTOR (C) from Western blots in (A). (D) RT-qPCR analysis of *mTOR* mRNA expression. Data were the mean ± SE (n = 3). Different letters marked above values indicate significant differences ($p < 0.05$).

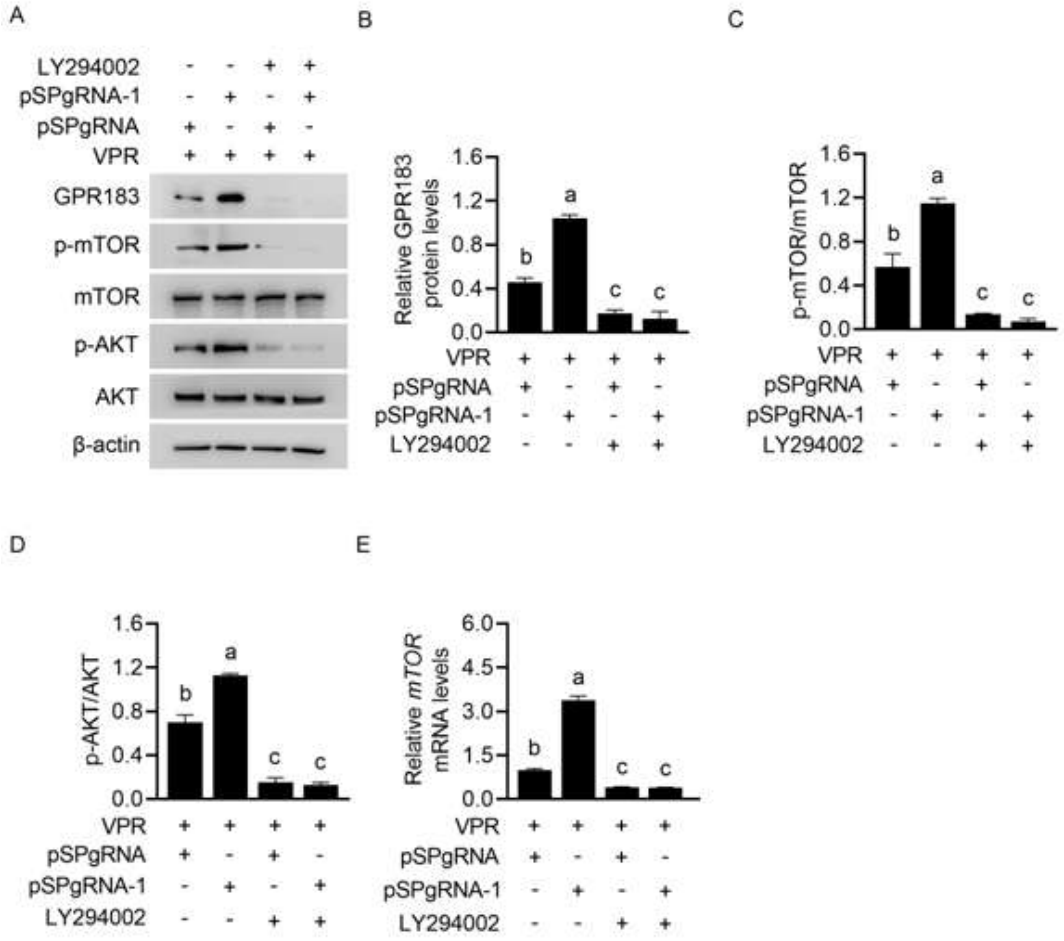

Figure 11. Effect of PI3K inhibition on GPR183-stimulated mTOR mRNA expression and phosphorylation.

(A) HC11 cells were transfected with pSPgRNA-1 and treated with LY294002 for 48 h. Indicated protein levels were detected by Western blotting. (B-D) Quantification by ImageJ of GPR183/*β*-actin (B), p-mTOR/mTOR (C), and p-AKT/AKT (D) from Western blots in (A). (E) RT-qPCR analysis of *mTOR* mRNA expression.

Figure S1. Effect of Met on mTOR phosphorylation

(A) HC11 cells were treated with Met (0.6 mM). Indicated protein levels were detected by Western blotting. (B) Quantification by ImageJ of p-mTOR/mTOR levels from Western blots in (A).

Figure S2. Cluster analysis of DEGs between blank and Met-treated group.

Cluster analysis of DEGs between blank and Met-treated group. Red indicated up-regulated DEGs and blue indicated down-regulated DEGs. The upper part was the dendrogram of sample clustering, and on the left was the dendrogram of gene clustering. Blank-1, 2, 3 represented three cell samples of blank group; Met-1, 2, 3, three cell samples of Met-treated group.

Figure S3. GO enrichment histogram of DEGs between the blank and Met-treated group

(A and B) GO enrichment histogram of upregulated (A) and downregulated (B) genes between the blank and Met (0.6 mM)-treated HC11 cells. The abscissa was the P value, and the ordinate was a simple description of the function entry. Function items were arranged in order of P value. Different color columns represented different classifications of GO terms. Red represented cell components; green, biological processes; and blue, molecular functions.